Theoretical Study of TiO-Catalyzed Hydrogenation of Carbon Dioxide to Formic Acid

Der-Yan Hwang*,† and Alexander M. Mebel*,‡

Department of Chemistry, Tamkang University, Tamsui 25137, Taiwan, and Department of Chemistry and Biochemistry, Florida International University, Miami, Florida 33199

Received: June 15, 2004; In Final Form: September 7, 2004

Density functional B3LYP/6-311+G(3df,2p)//B3LYP/6-31G(d,p) calculations have been performed for the potential energy surface of the $CO_2/H_2/TiO$ system. The results demonstrate that titanium oxide can serve as a catalyst for the gas-phase hydrogenation of carbon dioxide to formic acid. The most favorable reaction pathways are $CO_2 + H_2 + TiO(^3\Delta) \rightarrow H_2 + \eta^2\text{-}CO_2{-}TiO \rightarrow$ TS2 $\rightarrow \eta^2\text{-}CO_2{-}HTiOH \rightarrow$ TS3 $\rightarrow$ OC(H)OTiOH $\rightarrow$ TS4 $\rightarrow$ *cyc*-$HCO_2TiOH \rightarrow$ TS5 $\rightarrow$ cis-HOC(H)OTiO $\rightarrow$ *cis*-HCOOH + $TiO(^3\Delta)$ and (starting from the OC(H)OTiOH intermediate) OC(H)OTiOH $\rightarrow$ TS6 $\rightarrow$ *trans*-HC(O)O(H)TiO $\rightarrow$ *trans*-HCOOH + $TiO(^3\Delta)$. In these mechanisms, the highest relative energies with respect to the initial reactants are found for the final products, 7.4 and 11.0 kcal/mol for the trans and cis conformers of formic acid, respectively, and all transition states have lower energies. Therefore, in the gas phase, titanium oxide can be an efficient catalyst; the activation energy for the TiO-catalyzed hydrogenation of CO_2 coincides with its endothermicity. However, the highest barriers for individual reaction steps are lowered to 60.1 and 54.5 kcal/mol, respectively, as compared to 73.8 kcal/mol for the uncatalyzed $CO_2 + H_2 \rightarrow$ HCOOH reaction, indicating that in the condensed phase TiO would not be a particularly efficient catalyst.

1. Introduction

Carbon dioxide fixation is a significant problem that has received considerable attention in recent years[1−6] because of the environmental importance of CO_2 as a greenhouse gas and its large-scale availability at low cost. CO_2 is a highly oxidized and thermodynamically stable compound with low reactivity; therefore, its utilization remains a challenging task. These are the major reasons that toxic carbon monoxide instead of CO_2 is currently mostly used for many processes in industry as a C_1 building unit.[6] Homogeneous, heterogeneous, or enzymatic catalysis is a promising approach for CO_2 fixation. The homogeneous catalysis for CO_2 fixation has been discussed in recent reviews.[2,4] For instance, the catalytic hydrogenation of CO_2 to formic acid, which provides a prospective technique allowing the use of CO_2 as a raw material in large-scale chemical synthesis, has attracted much interest in recent years. Rhodium and ruthenium phosphine complexes were found to act as efficient catalysts for the formation of formic acid from CO_2.[7−9]

Alternatively, heterogeneous catalysis can provide several technical advantages due to stability, separation, handling, and reuse of the catalyst and reactor design. However, at present, the range of compounds that have been synthesized from CO_2 by heterogeneous catalytic methods is still relatively narrow; these methods are mainly confined to methanol synthesis, the syntheses of methylamines and formic acid derivatives, and the production of synthesis gas.[6] For example, a ruthenium-containing silica hybrid catalyst has been suggested for the production of various derivatives of formic acid.[6]

A search for new efficient catalysts for the fixation of carbon dioxide by H_2 to produce formic acid remains an active area of research. Metals and their compounds can catalyze many important chemical reactions, either homogeneously or heterogeneously. Transition-metal oxides can coordinate CO_2[10−12] and also react with molecular hydrogen.[13−15] From this point of view, it would be reasonable to expect that these oxides can assist the conversion of CO_2 to formic acid (i.e., catalyze the $CO_2 + H_2 \rightarrow$ HCOOH reaction, which is known to have a very high barrier without a catalyst[16−21]). In the present theoretical work, we use theoretical density functional calculations to investigate the reaction mechanism of carbon dioxide with H_2 catalyzed by TiO. We report the potential energy surface (PES) for this reaction, elucidate the gas-phase reaction mechanism, and provide geometric structures of various reactants, products, intermediates, and transition states as well as their reliable energies. This work continues our systematic studies of the reaction mechanisms of various chemical reactions, including the conversion of methane to methanol,[22−24] nitrogen hydrogenation,[25,26] and the conversion of CO to formaldehyde,[27] in the presence of metal oxides. A detailed understanding of the elementary reaction steps from reactants to the desired product and a comparison of the catalytic role of different transition-metal oxides would facilitate a rational design of potential catalysts.

2. Computational Details

Full geometry optimizations were run at the hybrid density functional B3LYP/6-31G(d,p) level of theory[28] to locate various stationary points (reactants, intermediates, transition states, and products) on the ground triplet electronic state PES of the $CO_2/H_2/TiO$ system. Harmonic vibrational frequencies were calculated at the same B3LYP/6-31G(d,p) level in order to characterize the stationary points as minima (number of imaginary frequencies NIMAG = 0) or first-order saddle points (NIMAG = 1), to obtain zero-point vibrational energy corrections (ZPE), and to generate force constants needed for intrinsic reaction coordinate (IRC)[29] calculations. The IRC method[29] was used

* E-mail: dyh@mail.tku.edu.tw.
† Tamkang University.
‡ Florida International University. E-mail: mebela@fiu.edu.

10.1021/jp047424q CCC: $27.50
Published on Web 10/16/2004

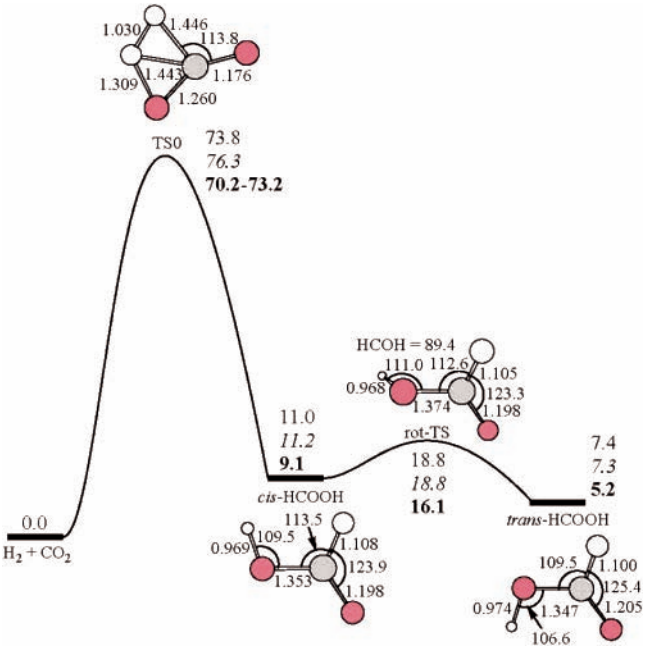

Figure 1. Potential energy diagram for the $H_2 + CO_2 \rightarrow$ HCOOH reaction without a catalyst. Relative energies of various species are given in kcal/mol; nonitalic and italic numbers are calculated at the B3LYP/6-311+G(3df,2p)//B3LYP/6-31G(d,p) + ZPE[B3LYP/6-31G(d,p)] and G2(MP2) (ref 21) levels of theory, respectively, and bold numbers show experimental energies. Optimized geometries of the reaction intermediates and transition states are also shown with bond lengths given in angstroms, and bond angles are given in degrees.

to track minimum-energy paths from transition structures to the corresponding minimum. The relative energies were refined using single-point calculations with B3LYP/6-31G(d,p)-optimized geometry employing B3LYP calculations with the larger 6-311+G(3df,2p) basis set. All density functional calculations described here were performed by employing the Gaussian 98 program.[30]

3. Results and Discussion

3.1. $CO_2 + H_2$ Reaction without a Catalyst. To validate the accuracy of the theoretical method chosen in this study, let us first consider the reaction of hydrogenation of CO_2 to formic acid without a catalyst. This reaction is the reverse of the decarboxylation of formic acid, which was investigated earlier both experimentally and theoretically by several groups.[16−21] The potential energy diagram for the $CO_2 + H_2 \rightarrow$ HCOOH reaction is illustrated in Figure 1. The hydrogenation process occurs in two steps: H_2 addition to CO_2 (or insertion of C═O into the H−H bond of molecular hydrogen) to form *cis*-HCOOH via transition state TS0 followed by cis−trans isomerization to produce the more stable *trans*-HCOOH structure. The barrier for the H_2 addition at TS0 calculated at the B3LYP/6-311+G(3df,2p)//B3LYP/6-31G(d,p) levels, 73.8 kcal/mol, is close to the range estimated from experiment, 70.2−73.2 kcal/mol,[17,18] and underestimates the G2(MP2) value by 2.5 kcal/mol.[21] The relative energies of the other structures, *cis*- and *trans*-HCOOH, and the rotational transition states are very close at the B3LYP and G2(MP2) levels of theory and systematically overestimate the experimental energies by about 2 kcal/mol, which is related to the overestimation of the experimental energy difference between $CO_2 + H_2$ and formic acid. We can conclude that the B3LYP method chosen here for the study of the $CO_2 + H_2$ reaction catalyzed by TiO should be reliable because this density functional approach is also usually reasonably accurate for transition-metal compounds.[14,31−33]

3.2. $CO_2 + H_2$ Reaction in the Presence of TiO. Here we consider the lowest-energy triplet electronic state for the $CO_2 + H_2 + TiO(^3\Delta)$ reaction. The total energies, ZPE, and relative energies of various reactants, products, intermediates, and transition states for this reaction are presented in Table 1; their vibrational frequencies are shown in Table 2. The potential energy diagram along the $CO_2 + H_2 + TiO(^3\Delta) \rightarrow$ HCOOH + $TiO(^3\Delta)$ reaction pathway is illustrated in Figure 2, and the optimized geometries of the intermediates and transition states are depicted in Figure 3.

3.2.1. H_2 and CO_2 Addition to Titanium Oxide. At the initial stage, two different reaction scenarios are possible. In the first one, titanium oxide reacts with molecular hydrogen and then with CO_2, and in the second mechanism, the reaction sequence is the opposite: TiO first reacts with carbon dioxide and then with H_2. We considered the $TiO(^3\Delta) + H_2$ reaction earlier[34] and found that titanium oxide can insert into the H−H bond via a planar transition state TS1 overcoming a moderate 16.9 kcal/mol barrier. As a result, the planar C_s-symmetric HTiOH ($^3A''$) molecule is produced, and the reaction is calculated to be 12.6 kcal/mol exothermic. HTiOH can form a rather strong complex with carbon dioxide, η^2-CO_2−HTiOH, bound by 12.3 kcal/mol with respect to separated HTiOH and CO_2 molecules. This complex is formed without a barrier, and it resides 24.9 kcal/mol lower in energy than the initial reactants. The structure of η^2-CO_2−HTiOH is nonplanar and has a side-on orientation of a C═O bond of CO_2 with respect to the transition-metal atom.

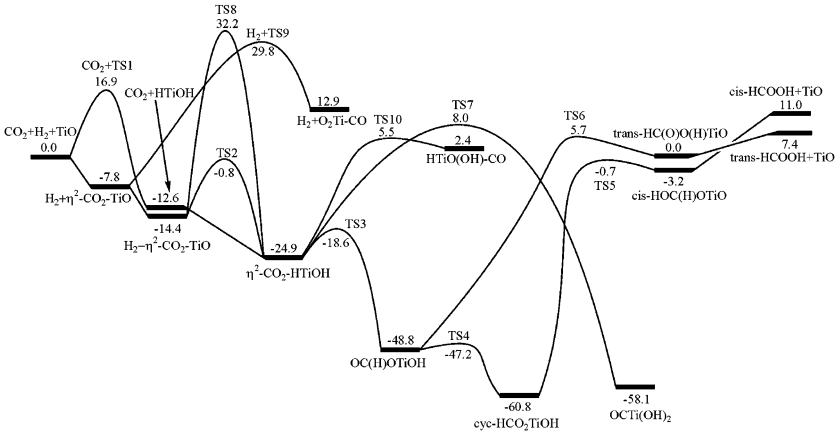

Figure 2. Potential energy diagram for the $CO_2 + H_2 + TiO(^3\Delta) \rightarrow$ HCOOH + $TiO(^3\Delta)$ reaction calculated at the B3LYP/6-311+G(3df,2p)//B3LYP/6-31G(d,p) + ZPE[B3LYP/6-31G(d,p)] level. Relative energies of various species are given in kcal/mol.

TABLE 1: Total Energies (hartrees), ZPE, and Relative Energies (kcal/mol) of Various Species in the $CO_2 + H_2 + TiO$ Reaction Calculated at the B3LYP/6-31G(d,p) and B3LYP/6-311+G(3df,2p)//B3LYP/6-31G(d,p) Levels of Theory

	B3LYP/6-31G(d,p)			B3LYP/6-311+G(3df,2p)	
species	total energy	ZPE	relative energy	total energy	relative energy
H_2	−1.17854	6.39		−1.18001	
CO_2	−188.58094	7.28		−188.65985	
$H_2 + CO_2$	−189.75948	13.66	0	−189.83986	0
TS0	−189.64474	15.12	73.46	−189.72456	73.81
trans-HCOOH	−189.76222	21.33	5.95	−189.84022	7.45
cis-HCOOH	−189.75410	21.07	10.79	−189.83409	11.03
rot-TS	−189.73972	19.98	18.72	−189.81994	18.81
TiO ($^3\Delta$)	−924.61450	1.57		−924.70036	
$TiO + H_2$	−925.79304	7.96	0	−925.88037	0
TS1	−925.76474	9.48	19.28	−925.85583	16.92
HTiOH	−925.81314	10.73	−9.84	−925.9049	−12.62
$CO_2 + H_2 + TiO$	−1114.37398	15.23	0	−1114.54022	0
CO_2 + HTiOH	−1114.39408	18.01	−9.84	−1114.56475	−12.62
η^1-CO_2−HTiOH	−1114.41589	17.79	−23.74	−1114.57623	−20.04
η^2-CO_2−HTiOH	−1114.42502	18.45	−28.81	−1114.58507	−24.93
η^1-CO_2−TiO	−1113.20491	9.08		−1113.36626	
$H_2 + \eta^1$-CO_2−TiO	−1114.38345	15.46	−5.71	−1114.54627	−3.57
η^2-CO_2−TiO	−1113.21387	8.67		−1113.37233	
$H_2 + \eta^2$-CO_2−TiO	−1114.39241	15.05	−11.74	−1114.55234	−7.79
H_2-η^2-CO_2−TiO	−1114.41076	18.60	−19.71	−1114.56860	−14.44
TS2	−1114.38570	17.10	−5.48	−1114.54440	−0.75
TS3	−1114.41266	18.20	−21.30	−1114.57466	−18.64
OC(H)OTiOH	−1114.46423	22.53	−49.34	−1114.62962	−48.80
TS4	−1114.46355	22.59	−48.85	−1114.62712	−47.17
cyc-HCO_2TiOH	−1114.48644	22.72	−63.08	−1114.64904	−60.79
TS5	−1114.39329	22.17	−5.18	−1114.55236	−0.68
cis-HOC(H)OTiO	−1114.39896	22.92	−7.99	−1114.55759	−3.21
TS6	−1114.38187	20.57	0.39	−1114.53968	5.68
trans-HC(O)O(H)TiO	−1114.39317	23.41	−3.869	−1114.55319	0.04
TS7	−1114.36882	16.68	4.68	−1114.52982	7.97
$OCTi(OH)_2$	−1114.47145	20.08	−56.31	−1114.64046	−58.05
TS8	−1114.33126	13.63	25.20	−1114.48639	32.17
TS9	−1113.15281	6.89		−1113.30954	
H_2 + TS9	−1114.33135	13.27	24.79	−1114.48955	29.84
O_2Ti−CO	−1113.18217	7.12		−1113.33691	
$H_2 + O_2$Ti−CO	−1114.36071	13.50	6.60	−1114.51692	12.89
TS10	−1114.37425	16.33	0.93	−1114.53320	5.50
HTiO(OH)−CO	−1114.38017	16.82	−2.30	−1114.53887	2.44
TiO + *trans*-HCOOH	−1114.37672	22.90	5.95	−1114.54058	7.45
TiO + *cis*-HCOOH	−1114.36860	22.64	10.79	−1114.53445	11.03

The coordinated C═O bond is elongated by 0.11 Å as compared to that in the isolated CO_2 molecule, whereas the second C═O bond is lengthened slightly, only by 0.03 Å. The CO_2 fragment loses its linearity, and the OCO angle in the complex is 143.1°. The bonding between the fragments in η^2-CO_2−HTiOH can be described in terms of electron donation from the bonding p_π molecular orbital (MO) of CO_2 to a d_σ orbital of Ti and back donation from a singly occupied d_δ orbital of the metal atom to the antibonding p_π* MO of CO_2. HTiOH and CO_2 can also form an end-on η^1-CO_2−HTiOH complex bound by 7.4 kcal/mol. This complex lies 20.0 kcal/mol below the initial reactants but is 4.9 kcal/mol less stable than η^2-CO_2−HTiOH. The deformation of the CO_2 fragment in η^1-CO_2−HTiOH is more significant than in η^2-CO_2−HTiOH; the end-on coordinated C−O bond is stretched to 1.309 Å, and the OCO angle decreases to 131.6°. The end-on complex is not relevant for the CO_2 hydrogenation reaction pathway because the H shift from Ti to C triggering that reaction involves η^2-CO_2−HTiOH rather than η^1-CO_2−HTiOH (section 3.2.2).

In the alternative mechanism, TiO initially forms a side-on η^2-CO_2−TiO complex with carbon dioxide without a barrier. The binding energy for this complex, 7.8 kcal/mol with respect to TiO + CO_2, is lower than that for η^2-CO_2−HTiOH. This result correlates with the fact that the Ti−O and Ti−C bond distances in η^2-CO_2−TiO, 2.071 and 2.340 Å, respectively, are significantly longer than those in η^2-CO_2−HTiOH, 2.019 and 2.276 Å, respectively. Meanwhile, the geometries of the CO_2 fragment in the two complexes are very similar. The end-on η^1-CO_2−TiO complex can also exist. It is calculated to be bound by 3.6 kcal/mol with respect to TiO and CO_2 (i.e., twice as weakly bound as the side-on η^2-CO_2−TiO). The deformation of the CO_2 fragment in η^1-CO_2−TiO is insignificant; the coordinated C−O bond elongates by only 0.02 Å as compared to that in free carbon dioxide, and the fragment remains nearly linear (Figure 3). Similar to η^1-CO_2−HTiOH, η^1-CO_2−TiO does not play any role in the reaction mechanism. However, the η^2-CO_2−TiO complex can in turn form another complex with molecular hydrogen, H_2-η^2-CO_2−TiO, which also exhibits the side-on orientation of the H_2 fragment relative to the Ti atom. The H_2 and CO_2 fragments interact with different d orbitals of the metal and therefore lie in different planes; the dihedral TiHHO angle is 106.1°. The structure of the CO_2 fragment is nearly the same as those in η^2-CO_2−TiO and η^2-CO_2−HTiOH, whereas the H−H bond is stretched by about 0.04 Å as compared to that in free molecular hydrogen. The binding energy of H_2-η^2-CO_2−TiO is calculated to be 6.6 kcal/mol with respect to η^2-CO_2−TiO + H_2 and 14.4 kcal/mol relative to the three separated reactants, $CO_2 + H_2 + TiO(^3\Delta)$. Both reaction steps from the reactants to the three-fragment complex are barrierless. The H_2-η^2-CO_2−TiO intermediate rearranges into the η^2-CO_2−HTiOH complex by the insertion of TiO into the H−H bond via TS2. The TiO−H_2 fragment in transition state

TABLE 2: Vibrational Frequencies (cm^{-1}) of Various Compounds in the $CO_2 + H_2 + TiO$ Reaction Calculated at the B3LYP/6-31G(d,p) Level

species	frequencies
TS1	1473i, 932, 985, 1124, 1594, 1986
HTiOH	301, 440, 478, 767, 1581, 3917
η^1-CO_2−HTiOH	43, 74, 102, 166, 206, 291, 345, 405, 572, 737, 839, 1166, 1672, 1875, 3949
η^2-CO_2−HTiOH	82, 121, 204, 261, 303, 340, 408, 420, 538, 707, 822, 1165, 1647, 1954, 3947
η^1-CO_2−TiO	31, 34, 103, 187, 539, 574, 1077, 1363, 2442
η^2-CO_2−TiO	71, 146, 212, 371, 403, 678, 1072, 1161, 1947
H_2-η^2-CO_2−TiO	91, 158, 164, 266, 292, 400, 438, 688, 698, 779, 1081, 1173, 1216, 1940, 3624
TS2	1347i, 82, 150, 174, 236, 387, 413, 697, 950, 992, 1129, 1167, 1655, 1947, 1985
TS3	657i, 69, 100, 256, 342, 372, 379, 449, 571, 709, 769, 1152, 1634, 2029, 3919
OC(H)OTiOH	36, 56, 127, 159, 432, 437, 485, 744, 790, 1055, 1248, 1415, 1805, 2991, 3957
TS4	111i, 39, 80, 173, 429, 433, 511, 738, 782, 1060, 1247, 1402, 1752, 3014, 3946
cyc-HCO_2TiOH	78, 78, 233, 313, 364, 391, 420, 769, 827, 1066, 1344, 1398, 1594, 3057, 3961
TS5	464i, 86, 140, 163, 348, 449, 612, 792, 1030, 1105, 1177, 1318, 1442, 3059, 3794
cis-HOC(H)OTiO	86, 121, 147, 293, 399, 458, 614, 753, 1050, 1109, 1253, 1341, 1548, 3051, 3806
TS6	1305i, 50, 125, 161, 304, 539, 712, 995, 1046, 1183, 1205, 1411, 1788, 1860, 3010
trans-HC(O)O(H)TiO	40, 46, 114, 167, 201, 633, 683, 1030, 1064, 1092, 1239, 1402, 1874, 3104, 3687
TS7	394i, 90, 134, 247, 296, 357, 402, 415, 446, 531, 721, 763, 1270, 2055, 3938
$OCTi(OH)_2$	83, 94, 138, 244, 247, 281, 311, 316, 366, 402, 735, 810, 2051, 3972, 3975
TS8	199i, 97, 180, 220, 287, 316, 385, 425, 489, 649, 715, 1078, 1172, 1438, 2081
TS9	457i, 80, 161, 263, 309, 343, 556, 1030, 2078
O_2Ti−CO	46, 90, 179, 284, 306, 379, 576, 1030, 2088
TS10	191i, 65, 147, 206, 242, 286, 308, 374, 416, 503, 703, 779, 1315, 2122, 3957
HTiO(OH)−CO	74, 87, 161, 197, 279, 307, 336, 359, 412, 474, 644, 778, 1637, 2117, 3903

TS2 has a very similar structure to that of TS1. Small differences between the two indicate that TS2 has a slightly earlier character than TS1; the breaking H−H bond is somewhat shorter, 1.046 Å in TS2 versus 1.069 Å in TS1, and the forming Ti−H and O−H bonds are longer, 1.879 and 1.282 Å in TS2 versus 1.871 and 1.254 Å in TS1, respectively. Although the CO_2 fragment seems to play only a spectator role in the insertion of titanium oxide into H_2, its presence results in a small decrease of the reaction exothermicity, from 12.6 kcal/mol without CO_2 to 10.5 kcal/mol with CO_2, and a notable reduction of the reaction barrier from 16.9 to 13.6 kcal/mol. Owing to this barrier decrease and to the fact that the H_2-η^2-CO_2−TiO complex is significantly bound with respect to the initial reactants, transition state TS2 lies 0.8 kcal/mol below $CO_2 + H_2 + TiO(^3\Delta)$. Therefore, the $CO_2 + H_2 + TiO(^3\Delta) \rightarrow H_2 + \eta^2$-$CO_2$−TiO $\rightarrow H_2$-η^2-CO_2−TiO $\rightarrow$ TS2 $\rightarrow \eta^2$-CO_2−HTiOH reaction is expected to be fast (all intermediates and the transition state are lower in energy than the reactants), and the η^2-CO_2−HTiOH complex can be readily produced. The $CO_2 + H_2 + TiO(^3\Delta) \rightarrow H_2 + \eta^2$-$CO_2$−TiO $\rightarrow H_2$-η^2-CO_2−TiO $\rightarrow$ TS2 $\rightarrow \eta^2$-CO_2−HTiOH mechanism for the formation of the η^2-CO_2−HTiOH intermediate is clearly preferable as compared to the "H_2 first, then CO_2" pathway, $CO_2 + H_2 + TiO(^3\Delta) \rightarrow$ TS1 $\rightarrow CO_2 +$ HTiOH $\rightarrow \eta^2$-CO_2−HTiOH, because for the latter the barrier of 16.9 kcal/mol relative to the initial reactants has to be overcome.

3.2.2. Formation of Formic Acid. η^2-CO_2−HTiOH can readily isomerize to the planar OC(H)OTiOH intermediate by 1,3-hydrogen migration from Ti to the C atom via TS3. The barrier for this process is calculated to be as low as 6.3 kcal/mol, and the transition state resides 18.6 kcal/mol below the initial reactants. TS3 has a four-membered ring TiHCO fragment and exhibits very early character with the breaking Ti−H bond only 0.01 Å longer than that in the η^2-CO_2−HTiOH reactant and the forming C−H bond of 2.003 Å nearly 0.9 Å longer than that in the reaction product. After the barrier at TS3 is cleared, the COTi angle eventually increases from 82.8 to 151.5°, the Ti−C bond (2.251 Å in the transition state) completely breaks apart, and the molecule takes a planar shape. The connections from TS3 to η^2-CO_2−HTiOH and OC(H)OTiOH in the forward and reverse directions, respectively, have been confirmed by IRC calculations. The η^2-CO_2−HTiOH $\rightarrow$ OC(H)OTiOH reaction step is calculated to be 23.9 kcal/mol exothermic, and the OC(H)OTiOH intermediate lies 48.8 kcal/mol lower in energy than the $CO_2 + H_2 + TiO(^3\Delta)$ reactants.

From OC(H)OTiOH, the reaction can proceed by two alternative pathways. First, this intermediate can undergo a facile ring closure to form the *cyc*-HCO_2TiOH molecule, which includes a TiOCO four-membered ring fragment. Five atoms, H, O, Ti, C, and H, in this structure lie on the same straight line, and the molecule is C_{2v}-symmetric. The energy of *cyc*-HCO_2TiOH is 60.8 kcal/mol lower than the energy of the initial reactants, and this structure represents the most favorable isomer in the $CO_2/H_2/TiO$ system among all local minima found in this study. The barrier for the ring closure is calculated to be very low, only 1.6 kcal/mol relative to the OC(H)OTiOH reactant; the corresponding transition state TS4 is 47.2 kcal/mol lower in energy than $CO_2 + H_2 + TiO(^3\Delta)$. The character of TS4 is rather early and reactantlike. The changes in the OC(H)OTiOH $\rightarrow$ *cyc*-HCO_2TiOH rearrangement mostly involve the TiOC angle, which decreases from 151.5° in the reactant to 120.5° in TS4 and to 88.1° in the product. Otherwise, the two C−O bonds (1.329 and 1.209 Å in OC(H)OTiOH and 1.322 and Å in TS4) become equal (1.272 Å) in the cyclic intermediate, and the TiOH fragment takes a linear arrangement. The next reaction step is 1,4-hydrogen transfer from TiO to an oxygen of the CO_2 fragment. According to the structure of the corresponding TS5 and results of IRC calculations, this process occurs by a rather peculiar pathway. From *cyc*-HCO_2TiOH to TS5, the initially planar molecule folds in such a way that the TiO fragment becomes almost perpendicular to the HCO_2 plane; the CO_2Ti dihedral angle is 100.2° in TS5. Then (but still before the transition state) the hydrogen atom migrates from TiO to the nearest oxygen of CO_2; in the transition state, this process is virtually completed, and the TiO−H and H−O distances are 2.707 and 0.969 Å, respectively. After the barrier at TS5 is cleared, the migrating hydrogen atom continues to move in the direction of the HCO_2 plane; this can also be described in terms of continuing rotation around the adjacent C−O bond. As a result of this complex rearrangement, the HOC(H)O fragment is produced in the cis configuration in terms of the position of two hydrogens. Thus, the isomerization product is a complex of TiO with the cis conformer of the formic acid molecule. The *cyc*-HCO_2TiOH $\rightarrow$ cis-HOC(H)OTiO reaction is highly endothermic, by 57.6 kcal/mol. The barriers at the late, productlike transition state TS5 are 60.1 and 2.5 kcal/mol in the forward and reverse directions, respectively. The complex is bound by 14.2 kcal/mol with respect to *cis*-HCOOH + TiO, which is close to the binding energy of η^2-CO_2−HTiOH (12.3 kcal/mol) but notably higher than that for η^2-CO_2−TiO (7.8 kcal/mol). Similar

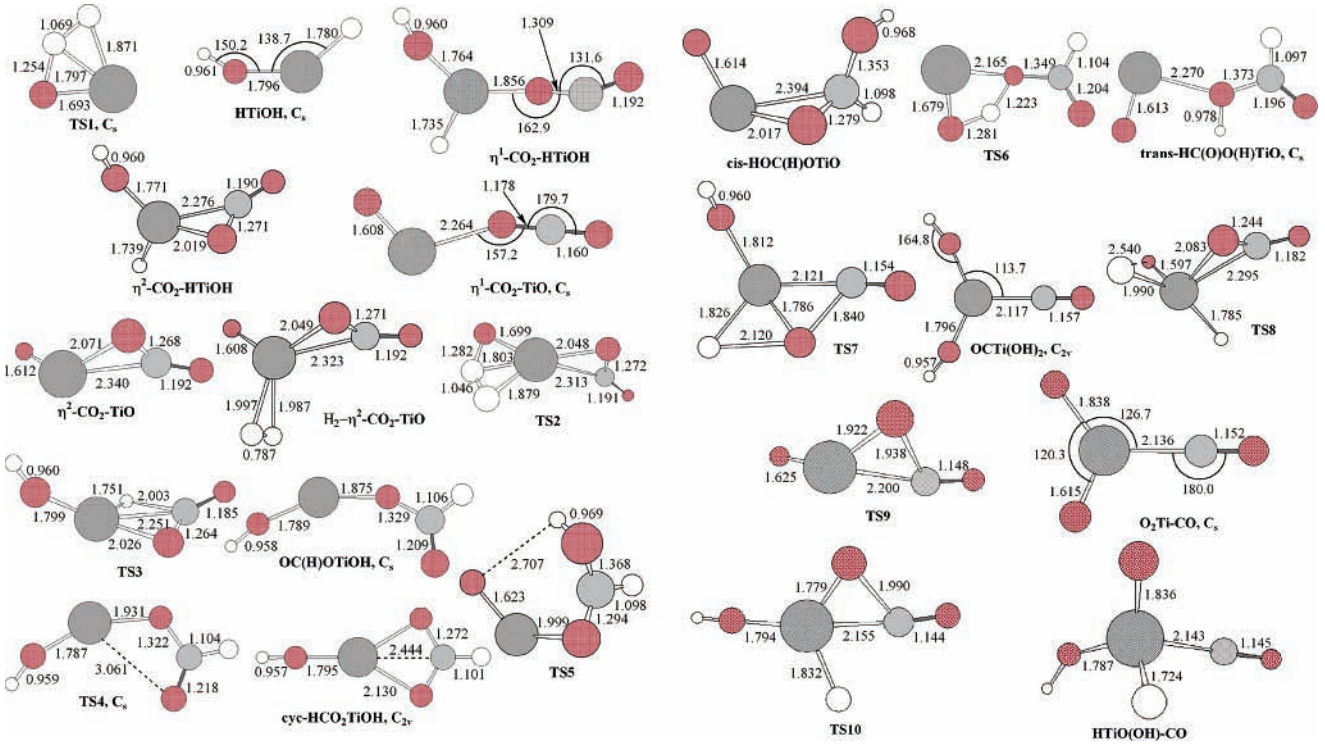

Figure 3. Geometries of various intermediates and transition states of the $CO_2 + H_2 + TiO(^3\Delta) \rightarrow HCOOH + TiO(^3\Delta)$ reaction optimized at the B3LYP/6-31G(d,p) level. Bond lengths are given in angstroms, and bond angles are given in degrees.

to η^2-CO_2−HTiOH and η^2-CO_2−TiO, *cis*-HOC(H)OTiO has a structure with a side-on (η^2) orientation of the double C═O bond of formic acid to the metal atom, and the geometries of the TiOC fragment in the three complexes are quite alike.

The second reaction pathway from the OC(H)OTiOH intermediate involves a 1,3-H shift via transition state TS6 between two oxygen atoms connected to TiO. In this case, the *trans*-HC(O)O(H)TiO complex of titanium oxide with the more stable trans conformer of formic acid is produced. The barrier for the hydrogen migration at TS6 is calculated to be 54.5 kcal/mol, and the resulting *trans*-HC(O)O(H)TiO molecule has similar energy to that of the initial $CO_2 + H_2 + TiO(^3\Delta)$ reactants. *trans*-HC(O)O(H)TiO is an end-on (η^1) complex bound by 7.4 kcal/mol, and it can dissociate to the final *trans*-HCOOH + TiO products without an exit barrier. The *cis*-HOC(H)OTiO and *trans*-HC(O)O(H)TiO structures differ not only by the conformation of the formic acid fragment and the orientation toward the Ti atom but also by the oxygen atom involved in Ti−O bonding, the C═O oxygen in the former and the hydroxyl oxygen in the latter. We also tried to find another transition state for the 1,5-H shift in OC(H)OTiOH between two terminal O atoms. However, in this case the search for a saddle point converged to transition state TS5, which, according to IRC calculations, connects *cyc*-HCO_2TiOH with *cis*-HOC(H)OTiO.

3.2.3. Other Reaction Mechanisms. Considering the η^2-CO_2−HTiOH complex, we can think of several pathways for the reaction to proceed that involve hydrogen migrations from the titanium and oxygen atoms of HTiOH to various atoms of carbon dioxide. We tried to find transition states for all six possibilities for the H transfer; however, the calculations gave us only two new transition states as compared to those described in the previous section. For instance, TS7 corresponds to the H migration process from Ti to the neighboring O atom, which is accompanied by the formation of the second Ti−O bond and cleavage of the C−O bond. This rearrangement can be also described as the insertion of the titanium atom into the coordinated C−O bond occurring in parallel with the hydrogen shift from Ti to O. The isomerization of η^2-CO_2−HTiOH via TS7 leads to the $OCTi(OH)_2$ molecule, which lies 58.1 kcal/mol lower in energy than the initial reactants. The barrier at TS7 is high, 32.9 kcal/mol relative to η^2-CO_2−HTiOH (i.e., 26.6 kcal/mol higher than the barrier at TS3 leading from the complex to the OC(H)OTiOH intermediate). Hence, the reaction channel leading to $OCTi(OH)_2$ is expected to be less probable than the channels producing the OC(H)OTiOH and *cyc*-HCO_2TiOH structures.

Saddle-point searches for the H transfers from the oxygen atom of HTiOH converged to transition state TS8. However, IRC calculations for TS8 demonstrated that this transition state has a different nature from those assumed when we tried to generate initial structures for geometry optimization. According to the IRC calculations, TS8 actually connects the H_2-η^2-CO_2−TiO complex with η^2-CO_2−HTiOH. The rearrangement via TS8 is peculiar: before the transition state, the H−H bond in the H_2 molecular fragment is broken, and the two hydrogen atoms form Ti−H bonds with the metal. However, this configuration (which can be called a TiH_2O−CO_2 complex) is not a local minimum but rather a saddle point. After the barrier at this structure is cleared, one of the H atoms transfers from Ti to the adjacent oxygen. As a result, TS8 corresponds to the same process as TS2; however, the barrier at the former, 46.6 kcal/mol relative to H_2-η^2-CO_2−TiO, is 33.0 kcal/mol higher than the barrier at the latter, and TS8 is not expected to play any role in the reaction. Meanwhile, these calculations showed that the H transfer from the O atom of the HTiOH fragment in η^2-CO_2−HTiOH would not compete with the H migration from Ti via TS3.

Earlier theoretical and experimental studies of the $Ti + CO_2$ reaction[33,35] have demonstrated that a bare titanium atom can easily insert into a C═O bond in carbon dioxide. In this view, we have also considered the possibility of a similar insertion of the metal atom in the TiO and HTiOH molecules into CO_2.

Our calculations show that such insertions could indeed take place; however, they are not energetically favorable. For instance, transition state TS9 connects the η^2-CO_2−TiO complex with the O_2Ti−CO molecule. In the transition state, one of the C═O bonds is being broken, because the C−O distance elongates to 1.938 Å, and a Ti−O bond is being formed (1.922 Å). The barrier at TS9 is high, 37.6 kcal/mol relative to η^2-CO_2−TiO, and the rearrangement of the complex to O_2Ti−CO is 20.7 kcal/mol endothermic and is not likely to occur. In the planar O_2Ti−CO molecule, which resides 12.9 kcal/mol higher in energy than TiO($^3\Delta$) + CO_2, the newly formed Ti−O bond is long (1.838 Å), and the old Ti−O bond maintains nearly the same bond length (1.615 Å) as compared to those in TiO($^3\Delta$) and η^2-CO_2−TiO. The insertion of the Ti atom of HTiOH into CO_2 also exhibits a high barrier, 30.4 and 18.1 kcal/mol relative to η^2-CO_2−HTiOH and CO_2 + HTiOH, respectively. The corresponding transition state TS10 lies 5.5 kcal/mol above the initial CO_2 + H_2 + TiO($^3\Delta$) reactants. TS10 is later transition state than TS9; the former has the longer breaking C−O bond (1.990 Å) and the shorter forming Ti−O bond (1.779 Å) as compared to those in the latter. The insertion results in a four-coordinated complex of the Ti atom, HTiO(OH)−CO, which lies 2.4 kcal/mol higher in energy than the initial reactants but is much less stable (by 50−60 kcal/mol) than the OC(H)OTiOH, *cyc*-HCO_2TiOH, and OCTi$(OH)_2$ molecules. HTiO(OH)−CO is also kinetically metastable because the reverse barrier at TS10 is only 3.1 kcal/mol. We can conclude that the η^2-CO_2−HTiOH → TS10 → HTiO(OH)−CO Ti-to-CO_2 insertion is not likely to compete with the η^2-CO_2−HTiOH → TS3 → OC(H)OTiOH hydrogen migration and would not give a significant contribution to the overall reaction mechanism.

4. Conclusions

Summarizing the reaction mechanisms described above, we can conclude that TiO can serve as a catalyst in the gas phase for the H_2 + CO_2 → HCOOH hydrogenation reaction of carbon dioxide to formic acid. The most favorable reaction pathways are the following: CO_2 + H_2 + TiO($^3\Delta$) → H_2 + η^2-CO_2−TiO → TS2 → η^2-CO_2−HTiOH → TS3 → OC(H)OTiOH → TS4 → *cyc*-HCO_2TiOH → TS5 → *cis*-HOC(H)OTiO → *cis*-HCOOH + TiO($^3\Delta$) and (starting from the OC(H)OTiOH intermediate) OC(H)OTiOH → TS6 → *trans*-HC(O)O(H)TiO → *trans*-HCOOH + TiO($^3\Delta$). Thus, TiO first forms a side-on complex with the carbon dioxide molecule, and then molecular hydrogen binds to this complex. Both complex-formation steps are exothermic and barrierless. After that, the TiO fragment inserts into the H−H bond over a low 13.6 kcal/mol barrier, and this is followed by the hydrogen migration from Ti to C to produce the OC(H)OTiOH intermediate, overcoming a barrier of only 6.3 kcal/mol. OC(H)OTiOH can easily rearrange to the cyclic *cyc*-HCO_2TiOH molecule, and the latter can isomerize to the *cis*-HOC(H)OTiO complex by the H shift from the O of TiOH to the O of CO_2. However, this step is endothermic, and a barrier of 60.1 kcal/mol has to be cleared. The *cis*-HOC(H)OTiO complex can decompose to TiO($^3\Delta$), and the cis conformer of formic acid, thus yielding the product and restoring the catalyst. The alternative reaction mechanism leads from OC(H)OTiOH to the *trans*-HC(O)O(H)TiO complex over a barrier of 54.5 kcal/mol, and then the complex dissociates to the trans conformer of formic acid and titanium oxide.

If the reaction occurs in the gas phase and the energy is slowly dissipated through collisions, then the reaction rate mostly depends on the activation barriers (relative energies of transitions states or products if the reaction steps have no barrier) with respect to the initial CO_2 + H_2 + TiO($^3\Delta$) reactants. For these conditions, the activation energy for the TiO-catalyzed hydrogenation of CO_2 simply coincides with its endothermicity, 7.4 and 11.0 kcal/mol for the trans and cis conformers, respectively, because all the transition states on the reaction pathways have lower energies than the products. In the condensed phase, where the collisional dissipation of energy is fast, the more important factors are barriers for individual reaction steps. The highest barriers calculated for the TiO-catalyzed CO_2 + H_2 → HCOOH reaction are 54.5 and 60.1 kcal/mol for the pathways leading to the trans and cis conformers of formic acid, respectively. These values are somewhat lower than the barrier for the noncatalyzed reaction, 73.8 kcal/mol at the same level of theory, but are significantly higher than the barriers found for the rhodium-catalyzed hydrogenation of CO_2.[9] This indicates that in the condensed phase titanium oxide would be a much less efficient catalyst than the organometallic compounds of Rh.[6−9] Meanwhile, the reaction mechanism described here may be typical for the catalysis of the CO_2 + H_2 → HCOOH reaction by other metal oxides, which can form complexes with CO_2 and then react with molecular hydrogen to produce HMOH−CO_2 complexes. Moreover, similar reaction motives can be relevant to the catalytic hydrogenation of CO_2 to formic acid on the surface of transition-metal oxides, and heterogeneous (gas−surface) catalysis can offer many advantages (including higher reaction temperature, stability, separation, handling, and reuse of the catalyst and reactor design) as compared to homogeneous catalysis in solution.

Our results also shed light on what products can be expected in matrix isolation experiments if the TiO, CO_2, and H_2 vapors are mixed together. According to the calculated potential energy surface, in addition to the binary η^1-CO_2−TiO and η^2-CO_2−TiO complexes and HTiOH molecule, the tertiary H_2-η^2-CO_2−TiO complex, the η^1-CO_2−HTiOH and η^2-CO_2−HTiOH complexes, and the *cyc*-HCO_2TiOH molecule can be easily produced, as well as OCTi$(OH)_2$, if the reaction conditions allow the 8.0 kcal/mol barrier at TS8 to be overcome. If the conditions are such that the energy of these molecules is not effectively dissipated through collisions, then formic acid and its complexes with TiO can be also formed.

Acknowledgment. We appreciate partial support from Tamkang University and Florida International University. Some of the computer equipment used in this study was supplied by the National Science Council of Taiwan, ROC.

Supporting Information Available: Details of IRC calculations. This material is available free of charge via the Internet at http://pubs.acs.org.

References and Notes

(1) Halmann, M. *Chemical Fixation of Carbon Dioxide: Methods for Recycling CO_2*; CRC Press: Boca Raton, FL, 1993.

(2) Behr, A. *Carbon Dioxide Activation by Metal Complexes*; VCH: Weinheim, Germany, 1988.

(3) *Enzymatic and Model Carboxylation and Reduction Reactions for Carbon Dioxide Utilization*; NATO ASI Series C; Aresta, M., Schloss, J. V., Eds.; Kluwer Academic Press: Dordrecht, The Netherlands, 1990; Vol. 314.

(4) Dinjus, E.; Fornika, R. Carbon Dioxide as C_1 Building Block. In *Applied Homogeneous Catalysis with Organometallic Compounds*; Cornils, B., Herrmann, W. A., Eds.; VCH: Weinheim, Germany, 1996; pp 1048−1072; Vol. 2.

(5) Aresta, M.; Quaranta, E.; Tommasi, I.; Giannoccaro, P.; Ciccarese, A. *Gazz. Chim. Ital.* **1995**, *125*, 509.

(6) Baiker, A. *Appl. Organomet. Chem.* **2000**, *14*, 751.

(7) Zhang, J. Z.; Li, Z.; Wang, H.; Wang, C. Y. *J. Mol. Catal. A: Chem.* **1996**, *112*, 9.

(8) Hutschka, F.; Dedieu, A.; Leitner, W. *Angew. Chem.* **1995**, *107*, 1905. Hutschka, F.; Dedieu, A.; Leitner, W. *Angew. Chem., Int. Ed. Engl.* **1995**, *34*, 1742.
(9) Hutschka, F.; Dedieu, A.; Eichberger, M.; Fornika, R.; Leitner, W. *J. Am. Chem. Soc.* **1997**, *119*, 4432.
(10) Tanabe, K. In *Catalysis, Science and Technology*; Anderson, J. R., Boudart, M., Eds.; Springer-Verlag: New York, 1981.
(11) Klabunde, K. J.; Kaba, R. A.; Morris, R. M. *Inorganic Compounds with Unusual Properties-II*; King, R. B., Ed.; Advances in Chemistry Series 173; American Chemical Society: Washington, DC, 1979.
(12) *Adsorption and Catalysis on Oxide Surfaces*; Che, M., Bond, G. C., Eds.; Studies in Surface Science and Catalysis 21; Elsevier: Amsterdam, 1985.
(13) Hwang, D.-Y.; Mebel, A. M. *Chem. Phys. Lett.* **2001**, *341*, 393.
(14) Mebel, A. M.; Hwang, D.-Y. *J. Phys. Chem. A* **2001**, *105*, 7460.
(15) Hwang, D.-Y.; Mebel, A. M. *J. Phys. Chem. A* **2002**, *106*, 520.
(16) Blake, P. G.; Davies, H. H.; Jackson, G. E. *J. Chem. Soc. B* **1971**, 1923.
(17) Hsu, D. S. Y.; Shaub, W. M.; Blackbum, M.; Lin, M. C. *The 19th International Symposium on Combustion*; The Combustion Institute: Pittsburgh, PA, 1983.
(18) Saito, K.; Kakamoto, T.; Kuroda, H.; Torii, S.; Imamura, A. *J. Chem. Phys.* **1984**, *80*, 4989.
(19) Goddard, J. D.; Yamaguchi, Y.; Schaefer, H. F., III. *J. Chem. Phys.* **1992**, *96*, 1158.
(20) Francisco, J. S. *J. Chem. Phys.* **1992**, *96*, 1167.
(21) Wang, B.; Hou, H.; Gu, Y. *Chem. Phys.* **1999**, *243*, 27.
(22) Hwang, D.-Y.; Mebel, A. M. *Chem. Phys. Lett.* **2001**, *348*, 303.
(23) Hwang, D.-Y.; Mebel, A. M. *Chem. Phys. Lett.* **2002**, *365*, 140.
(24) Hwang, D.-Y.; Mebel, A. M. *J. Phys. Chem. A* **2002**, *106*, 12072.
(25) Hwang, D.-Y.; Mebel, A. M. *J. Phys. Chem. A* **2003**, *107*, 5092.
(26) Hwang, D.-Y.; Mebel, A. M. *Chem. Phys. Lett.* **2003**, *375*, 17.
(27) Hwang, D.-Y.; Mebel, A. M. *J. Phys. Chem. A* **2001**, *105*, 10433.
(28) (a) Becke, A. D. *J. Chem. Phys.* **1993**, *98*, 5648. (b) Lee, C.; Yang, W.; Parr, R. G. *Phys. Rev. B* **1988**, *37*, 785.
(29) Gonzalez, C.; Schlegel, H. B. *J. Phys. Chem.* **1990**, *94*, 5523.
(30) Frisch, M. J.; Trucks, G. W.; Schlegel, H. B.; Scuseria, G. E.; Robb, M. A.; Cheeseman, J. R.; Zakrzewski, V. G.; Montgomery, J. A., Jr.; Stratmann, R. E.; Burant, J. C.; Dapprich, S.; Millam, J. M.; Daniels, A. D.; Kudin, K. N.; Strain, M. C.; Farkas, O.; Tomasi, J.; Barone, V.; Cossi, M.; Cammi, R.; Mennucci, B.; Pomelli, C.; Adamo, C.; Clifford, S.; Ochterski, J.; Petersson, G. A.; Ayala, P. Y.; Cui, Q.; Morokuma, K.; Malick, D. K.; Rabuck, A. D.; Raghavachari, K.; Foresman, J. B.; Cioslowski, J.; Ortiz, J. V.; Stefanov, B. B.; Liu, G.; Liashenko, A.; Piskorz, P.; Komaromi, I.; Gomperts, R.; Martin, R. L.; Fox, D. J.; Keith, T.; Al-Laham, M. A.; Peng, C. Y.; Nanayakkara, A.; Gonzalez, C.; Challacombe, M.; Gill, P. M. W.; Johnson, B. G.; Chen, W.; Wong, M. W.; Andres, J. L.; Head-Gordon, M.; Replogle, E. S.; Pople, J. A. *Gaussian 98*, revision A.7; Gaussian, Inc.: Pittsburgh, PA, 1998.
(31) Torrent, M.; Sola, M.; Frenking, G. *Chem. Rev.* **2000**, *100*, 439.
(32) Glukhovtsev, M. N.; Bach, R. D.; Nagel, C. J. *J. Phys. Chem. A* **1997**, *101*, 316.
(33) Hwang, D.-Y.; Mebel, A. M. *J. Chem. Phys.* **2002**, *116*, 5633.
(34) Hwang, D.-Y.; Mebel, A. M. *Chem. Phys.* **2004**, *304*, 301.
(35) Papai, I.; Mascetti, J.; Fournier, R. *J. Phys. Chem. A* **1997**, *101*, 4465.